Reactive Compatibilization of a Nitrile Rubber/Phenolic Resin Blend: Effect on Adhesive and Composite Properties

P. SASIDHARAN ACHARY, R. RAMASWAMY

Polymers and Special Chemicals Division, Vikram Sarabhai Space Centre, Thiruvananthapuram, 695022, India

Received August 1997; accepted 6 October 1997

ABSTRACT: Resole phenolic resins containing various *p*-cresol (PC) to phenol (P) mol ratios were prepared and characterized. These phenolic resins were blended with nitrile rubber (NBR) and the measurements of adhesive joint strength, stress–strain properties, DSC, TGA, DMA, TEM, and SEM were performed using a 50 : 50 NBR/phenolic resin blend. It was observed that the adhesive joint strength and the mechanical properties of the blend enhanced significantly on incorporation of *p*-cresol into the phenolic resin, and the optimum *p*-cresol/phenol mol ratio was in the vicinity of 2 : 1. Observation of a more continuous phase and the increase in T_g of the rubber region in the blend indicated increased reactivity and compatibilization of NBR with phenolic resin as *p*-cresol was incorporated. The effect of silica filler on the properties of the nitrile rubber/phenolic resin blend was also studied without and with *p*-cresol modification and the results suggest that silica filler take not only the role of a reinforcing filler in the nitrile–phenolic–silica composite, but also a role as surface compatibilizer of the blend components. © 1998 John Wiley & Sons, Inc. J Appl Polym Sci 69: 1187–2101, 1998

Key words: nitrile rubber/phenolic resin blend; *p*-cresol; phenol; reactive compatibilization; nitrile–phenolic adhesive

INTRODUCTION

Blending of polymers offers a means of producing new materials with tailored properties and has been extensively used in plastics, rubbers, composites, films, fibers, coatings, and adhesives.[1] Nitrile–phenolics developed in the early of 1950[2] by blending nitrile rubber (NBR) with thermosetting phenolic resins are used in the aerospace industry for structural bonding of metals and are still making a name for the excellent bond durability under severe environments.[3,4] Nitrile–phenolics also form adhesives for a variety of adherends such as rubbers, plastics, wood, paper products, glass, etc. In the automobile industry, they have been used to bond brake shoes and clutch disc assemblies. Nitrile rubber/phenolic resin blends also find applications in the preparation of high abrasion resistant tough moldings, O-rings, gaskets, cables, etc.[5] Nitrile rubber and phenolic resin possess unique properties individually and by their suitable combinations, characteristic properties of both can be utilized to obtain a wide variety of properties to meet specific requirements.[6–8]

Phenolic resins are stalwarts of the plastic industry and have shown considerable growth in aerospace industries due to their versatile properties.[9] The thermosetting resole type phenolics possess exceptional adhesive properties on metal surfaces and can form a relatively strong chemical bond by virtue of the complex formation of *O*-methyl hydroxyl phenol with the hydrated metal oxide surface.[10,11] Phenolics have high rigidity, dimensional stability, and exceptional heat and fire resistance due to the highly crosslinked aromatic structure and resonance-intensifying hydroxyl groups.

Correspondence to: P. S. Achary.

Journal of Applied Polymer Science, Vol. 69, 1187–2101 (1998)
 CCC 0021-8995/98/061187-15

The high brittleness and the cure shrinkage are the major drawbacks that hinder the widespread applications of phenolic resins. For most applications, they are modified by the inclusion of fibers, particulate fillers, or elastomeric materials to improve the resistance of the finished product to stress. The most established and commercially exploited method to improve toughness of the cured phenolics is blending with nitrile rubber. The nitrile rubber component in the system imparts elasticity and resilience, which helps to improve mechanical performance by absorbing energy through stress distribution and relief. Because the role of rubber in the blend is to modify the deformational behavior, the interactions between the nitrile rubber and phenolic resin at the interfacial zone have a dominant effect on the mechanical properties of the blend.

Wu[12] outlined that the main factors that determine the mechanical properties of the polymer blend are the mechanical strength of the bulk phases, the degree of phase separation, and adhesion between the two phases. In a previous article, we reported[13] that NBR and resole phenol formaldehyde (PF) resin, when mixed and cured, separate into two phases and form undesirably large domains with low adhesion between the phases that causes poor adhesive and mechanical properties. Our previous studies[13,14] have revealed that incorporation of *p*-cresol formaldehyde (PCF) into the PF/NBR blend results in a finer and a dispersed phase that when optimized provides useful improvements in adhesive and mechanical properties. PCF resin has intermediate polarity compared to NBR and PF resin, and can react faster with NBR than PF resin. Therefore, PCF molecules are likely to be concentrated at the PF/NBR interface and act as an external compatibilizing agent[15] and improve the compatibility and chemical bonding between NBR and PF resin. This article presents the results of a systematic study made on the mechanical, adhesive, thermal, and morphological properties of the cured phenolic resin/NBR blend (50 : 50) containing various *p*-cresol/phenol mol ratios in the phenolic resin. This article also deals with the effect of a silica filler on the properties of the NBR/phenolic resin blend composite without and with *p*-cresol modification. The results indicate that *p*-cresol that remains homogeneously distributed in the phenolic resin matrix is allowed to control the morphology of the blend and provides improved interfacial bonding between phenolic resin and NBR. The results reported herein further show that a silica filler takes not only the usual role of a reinforcing material in the blend, but also improves the compatibility of the blend.

EXPERIMENTAL

Materials

NBR used in this study was Perbunan NS 3307 (Bayer, Germany), which contains 33% acrylonitrile unit. Phenolic resins based on 0/1, 0.25/0.75, 0.5/0.5, 0.66/0.33, 0.75/0.25, and 1/0 mole ratios of PC/P (*p*-cresol/phenol), 1.5 mol of formaledehyde and 0.02 mol of NaOH catalyst were synthesized and used. Precipitated silica filler Tensil 33A (average particle size $< 20\ \mu$), obtained from Xerophils Baroda, India, was used as received. The other reagents used, were of commercial analytical grade.

Preparation of Phenolic Resins

PF resin, PCF resin, and four *p*-cresol phenol formaldehyde (PCPF) resins, based on PC/P mol ratio 0.25/0.75 (PCPF-a), 0.5/0.5 (PCPF-b), 0.66/0.33 (PCPF-c), and 0.75/0.25 (PCPF-d) were synthesized by the following general procedure.

Phenol (99%) and/or *p*-cresol (99%), formaldehyde solution (37%), and NaOH were added and heated at 60°C in a three-neck round-bottom flask, equipped with a water bath, reflux condenser, thermometer, and a stirrer. After stirring for 30 min at 60°C, the temperature was slowly raised to 80–85°C and maintained for 7 h. The phenolic resin formed was isolated by removing water at 60°C under reduced pressure (<10 mm/mg) using a rotary evaporator, until the water content was less than 2% (measured by volatile matter at 105°C). The composition of the phenolic resin was determined by ^{1}H-NMR and were further characterized by gel time, DSC, and TGA.

Blending and Curing Procedure

The nitrile–phenolics for this investigation were prepared by mixing 50 : 50 weight ratio of NBR/phenolic resin, vulcanizing agents (sulphur 1.5 phr, 2-mercapto benzothiazole 1.5 phr, ZnO 5 phr) and varied concentrations of silica filler on a two-roll open mill. The cure temperature of the blend was determined by DSC measurement, and the curing was carried out at 170 ± 2°C for 90 min at 5 MPa pressure in a hydraulic press.

Testing Methods

Gel time was determined for each phenolic resin by placing approximately 10 g of the resin in a test tube and heating in an oil bath at 170°C under continuous agitation. The time taken for the resin to become a soft elastic rubbery solid was measured using a stop watch.

^{1}H-NMR spectrum of the phenolic resin solution in $CD_3—CO—CD_3$ was recorded using a JEOL-FX90 Q instrument.

Differential scanning calorimetry (DSC) thermograms were obtained using a DuPont Thermal Analyzer with a 902 DSC cell at a heating rate of 10°C/min. A sample amount of 8–10 mg was used. The T_g was determined at the midpoint of the transition in heat capacity.

Thermogravimetric analysis (TGA) of the cured samples was carried out on a Dupont 951 thermal gravimetric analyzer in an N_2 atmosphere. The heating rate was 10°C/min. The weight of the sample was about 8–10 mg.

Lap shear, T-peel, and rubber (NBR)-to-metal peel test specimens were made according to ASTM-D-1002, ASTM-D-1876, and ASTM-D429B, respectively, according to the procedures described earlier[13,14] using a B51 SWP aluminum alloy. The metal surface was abraded with emery paper, cleaned with trichloroethylene, etched with $Na_2Cr_2O_7/H_2SO_4$ solution[16] at 65°C for 15 min, washed with water, and dried at 70°C for 2 h. The mixed nitrile–phenolic recipe was dissolved in MEK solvent to a 20% total solids solution and coated on the dried metal surface to give a thin film. The adhesive coated aluminium panels were air dried for 30 min, heated at 70°C for 30 min for complete evaporation of the solvent, assembled, and cured. Lap shear and T-peel strength measurements were performed at a crosshead speed of 10 mm/min and rubber (NBR)-to-metal peel strength at a crosshead speed of 50 mm/min using an Instron model 4202.

Stress–strain properties were measured using dumbbell specimens cut from cured films of approximately 1 mm thick, obtained by compression molding of the blend at 170 ± 2°C and 5 MPa pressure for 90 min. An Instron 4202, operating with a crosshead speed of 10 mm/min at room temperature, was employed for the tensile properties measurements.

Dynamic mechanical properties of the cured nitrile–phenolic blend were measured using Rheovibron. A vibration frequency of 35 Hz was applied to the test piece (20 mm length, 10 mm wide, 1 mm thick) from −100 to +100°C. The output data from the apparatus was recorded and calculated with a computer.

The extent of crosslinking of rubber in the blend was measured by a swelling test in methylene chloride at 25°C. In the calculation an interaction parameter value of 0.314 was used[17] for NBR at 25°C. The samples were immersed in methylene chloride to absorb the solvent for 1 week. After this, the samples were quickly taken up from the solvent, wiped, and weighed. The methylene chloride was then allowed to evaporate from the sample at room temperature for 2 days, after which the samples were again weighed. From these gravimetric results and density data for methylene chloride and nitrile rubber, and based on the assumption that swelling is negligible for the cured phenolic resin, the crosslink density of the rubber network was calculated using the Flory-Rhener equation[18]

$$\nu e = \frac{-1}{Vs} \frac{\ln(1 - Vr) + Vr + \kappa Vr^2}{Vr^{1/3} - Vr/2}$$

where νe is mol of network chain per unit volume, Vs is the volume of 1 mol of solvent, κ is the rubber–solvent interaction parameter, and Vr is the volume fraction of the rubber in the swollen sample determined using the relation[19]

$$Vr = \frac{\dfrac{D - FT}{\rho_r}}{\dfrac{D - FT}{\rho_r} + \dfrac{A_s}{\rho_s}}$$

where D is the deswollen weight of the specimen, T is the initial weight, F is the weight fractions of phenolic resin and filler, A_s is the weight of the solvent absorbed by the rubber, ρ_r is the density of rubber, and ρ_s is the density of the solvent.

Morphological studies were performed by means of transmission electron microscopy (TEM) and scanning electron microscopy (SEM). The specimens used for TEM were first fixed in OsO_4 solution and then cut into thin films with a microtone. TEM micrograph was obtained using an HITACHI A-8000 TEM operating at 75KV. SEM micrographs of the fractured surface of the tensile test specimens were obtained using a stereoscan 250 MK-3 Cambridge instrument. The specimen was cut and mounted on an aluminium stub using conductive silver paint and was sputter coated with a thin layer of gold before taking SEM.

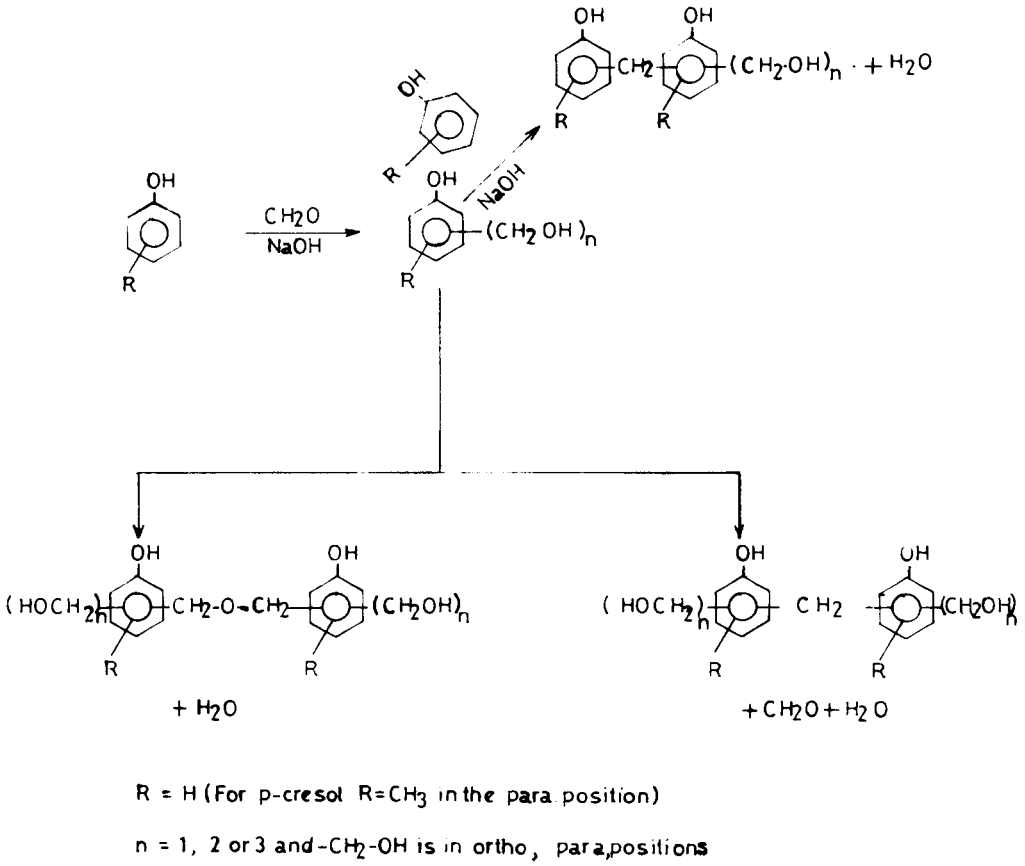

Figure 1 Mechanism of resole phenolic resin formation in a base-catalyzed reaction of phenol and formaldehyde.

RESULTS AND DISCUSSION

Phenol and *p*-cresol under alkaline conditions react with formaldehyde to produce methylol groups on the free ortho and para positions. Methylol groups further condense to form dinuclear and polynuclear phenols in which the phenolic nuclei are bridged by methylene or ether linkages,[20] as shown in Figure 1. With formaldehyde to a phenol mol ratio more than 1, methylol-terminated phenolic resins (resoles) are obtained. Under the assumption that *p*-cresol is more reactive towards formaldehyde than phenol and form dimethylol derivatives, we determined the *p*-cresol content in the phenolic resins based on ^{1}H-NMR integration of CH_3 and phenyl protons, and these are tabulated in Table I. The ^{1}H-NMR spectrum of a *p*-cresol phenol formaldehyde resin (PCPF-b) is shown in Figure 2, and the chemical shifts can be assigned as follows: 2 ppm ($-CH_3$), 3.7 ppm ($-CH_2-$ bridge), 4–5 ppm ($-CH_2-O-CH_2-$ or $-CH_2-OH$), 6–7 ppm (phenyl) protons.

To investigate the cure behavior of phenolic resins, DSC thermograms were recorded. As seen in Figure 3, the exothermic peak corresponding to the crosslinking reactions of the methylol group was observed in the DSC curve. The energy release detected by DSC does not yield the heat of reaction because of other thermal events like vaporization of the by products (H_2O and CH_2O) released during the cure reaction. Consequently, the heat evolution curve does not return to the baseline and the baseline for each trace was obtained by drawing the best smooth curve connecting the beginning and end. The exothermal heat of cure (ΔH), the temperature at which the first energy release is detected (T_1), the exothermal peak temperature (T_2), and the temperature indicating the end of exotherm (T_3) for various phenolic resins are given in Table I. Slow down of cure reaction with the increase of *p*-cresol content is demonstrated by the DSC data and gel time (Table I). The hardening reactions[21] of resole phenolic resins by heat is known to occur by the steps

Table I Composition, Geltime, DSC, TGA Data of Phenolic Resins

Sample Designation	*p*-Cresol/Phenol Mol Ratio Determined by ^{1}H-NMR	Geltime at 170°C (s)	DSC Data (Cure)				TGA Data of Cured Phenolic Resins in N_2 Atmosphere			
			T_1 (°C)	T_2 (°C)	T_3 (°C)	ΔH J/g	T_i (°C)	T_{max} (°C)	T_f (°C)	Residue at 900°C (%)
PF	0/1	148	110	156	178	100.2	390	520	640	62.2
PCPF-a	0.245/0.755	152	122	162	185	81.2	370	530	630	59.0
PCPF-b	0.490/0.510	159	127	167	184	52.2	360	510	590	56.5
PCPF-c	0.659/0.340	220	131	174	197	42.2	360	511	580	56.0
PCPF-d	0.733/0.267	269	150	175	202	37.9	350	410	560	54.1
PCF	1/0	370	162	185	200	26.1	330	360	500	45.2

shown in Figure 6(A). The retarding effect of cure by *p*-cresol is probably because *p*-alkyl substitution yield quinone methide with ease, and its increasing proportion will result in slow down of the condensation steps. On the basis of the DSC data, it was decided to cure various compositions for this study at 170°C.

Thermal stability of various phenolic resins

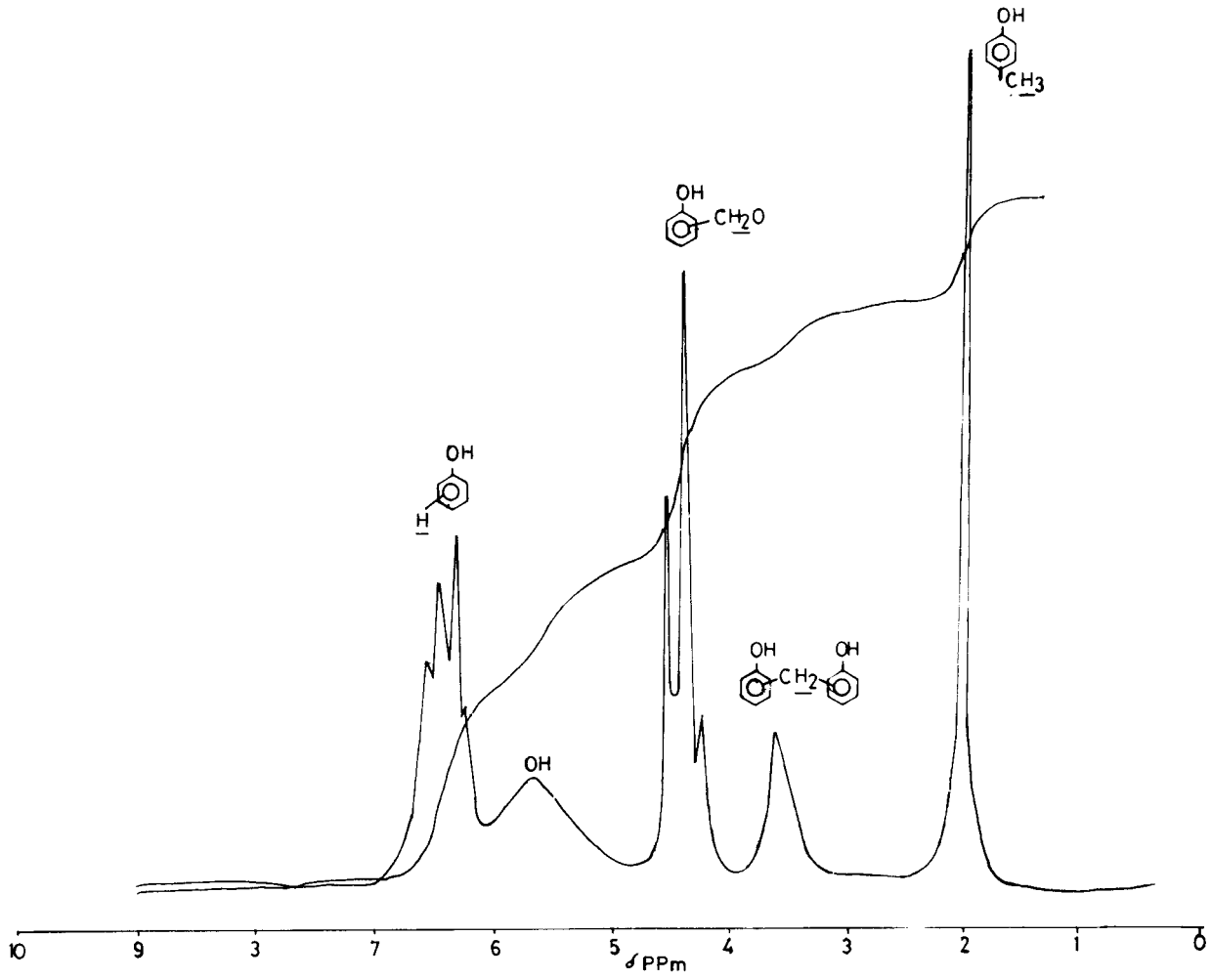

Figure 2 ^{1}H-NMR spectrum of *p*-cresol phenol formaldehyde (PCPF-b) resole resin.

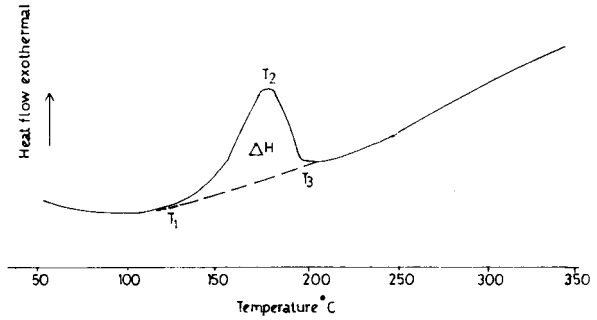

Figure 3 DSC trace for curing of *p*-cresol phenol formaldehyde (PCPF-b).

cured at 170°C for 90 min was evaluated by thermogravimetric analysis. Figure 4 shows the TG-DTG thermograms of a *p*-cresol phenol formaldehyde resin (PCPF-b). The relative thermal stabilities of the cured phenolics were assessed by comparison with initial decomposition temperature (T_i), the temperature of maximum rate of weight loss (T_{max}), the final decomposition temperature (T_f), and residue at 900°C. The results obtained are summarized in Table I, which show that as *p*-cresol content in the phenolic resin increased, the thermal stability of the cured resin decreased, because of the presence of difunctional *p*-cresol in the place of trifunctional phenol.

Reactions That Can Occur During the Cure of the Nitrile–Phenolic Blend

DSC trace for a freshly mixed nitrile–phenolic blend is shown in Figure 5(a), which indicated an exothermic peak corresponding to the cure reactions. The same mix that was kept at 170°C for 90 min at 5 MPa pressure showed no residual cure exotherm (RCE) in the DSC thermogram [Fig. 5(b)], which clearly indicated a complete cure. It is believed that three types of chemical reactions are possible during the cure (a) self-hardening of phenolic resin, (b) interlinking of phenolic resin with rubber, and (c) vulcanization of rubber.

Zinke[22] showed that the hardening mechanism of resole phenolic resin by heat involves a $—CH_2—O—CH_2$ bridge formation up to 160°C, and above this temperature the ether bridges begin to convert to methylene bridges. There is spectroscopic evidence for a quinone methide structure[23] during the heating of the phenolic resin above 160°C. It is likely that the quinone methide intermediate undergoes various chemical reactions to produce stable forms, as shown in Figure 6(A). Greeth[24] and Huttzsch[25] believed that *O*-methylene quinone methide reacts with the rubber double bond to form a chroman structure via Diel's Alder type 1,4 cyclo addition [Fig. 6(B)]. Van der Meer[26] proposed an "ene" mechanism that involves the abstraction of an alkyl hydrogen from the unsaturated rubber by the quinone methide intermediate. R. P. Lattimer et al.[27] provided evidence for a chroman structure and against the allyl hydrogen "ene" mechanism.

The chemistry of sulphur vulcanization of rubber is complex, and it is believed that the reaction proceeds through allylic hydrogen, as shown in Figure 6(C).

Stress–Strain Properties

The stress–strain curves of the cured phenolic resin/NBR (50 : 50) blends containing various *p*-cresol/phenol mol ratios in the phenolic resin are shown in Figure 7. It can be observed that incorporation of *p*-cresol into the phenolic resin has provided improvement in modulus and tensile strength. Moreover, as the *p*-cresol is used to replace phenol, the elongation at break decreases, in spite of the low functionality of the *p*-cresol compared with phenol. *p*-Cresol increases the energy-absorbing efficiency, and the best balance of properties are obtained in the vicinity of a *p*-cresol/phenol mol ratio of 2 : 1 (PCPF-c), as shown in Table II.

Because the mechanical properties of the blend depend on the interfacial adhesion between the blend components and the microdomain charac-

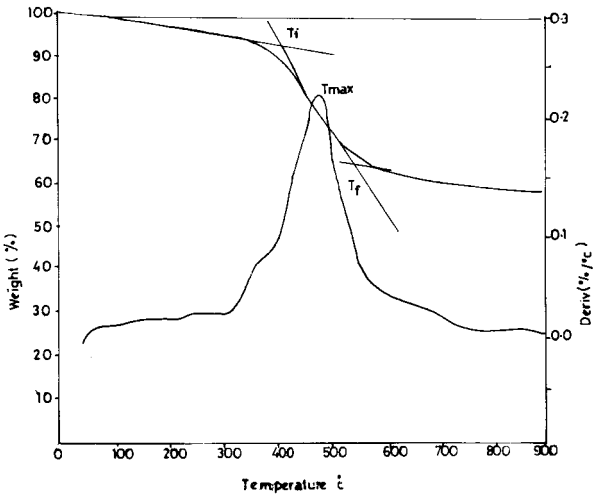

Figure 4 TG-DTG thermograms of cured *p*-cresol phenol formaldehyde (PCPF-b) in N_2 atmosphere (heating rate 10°C/min).

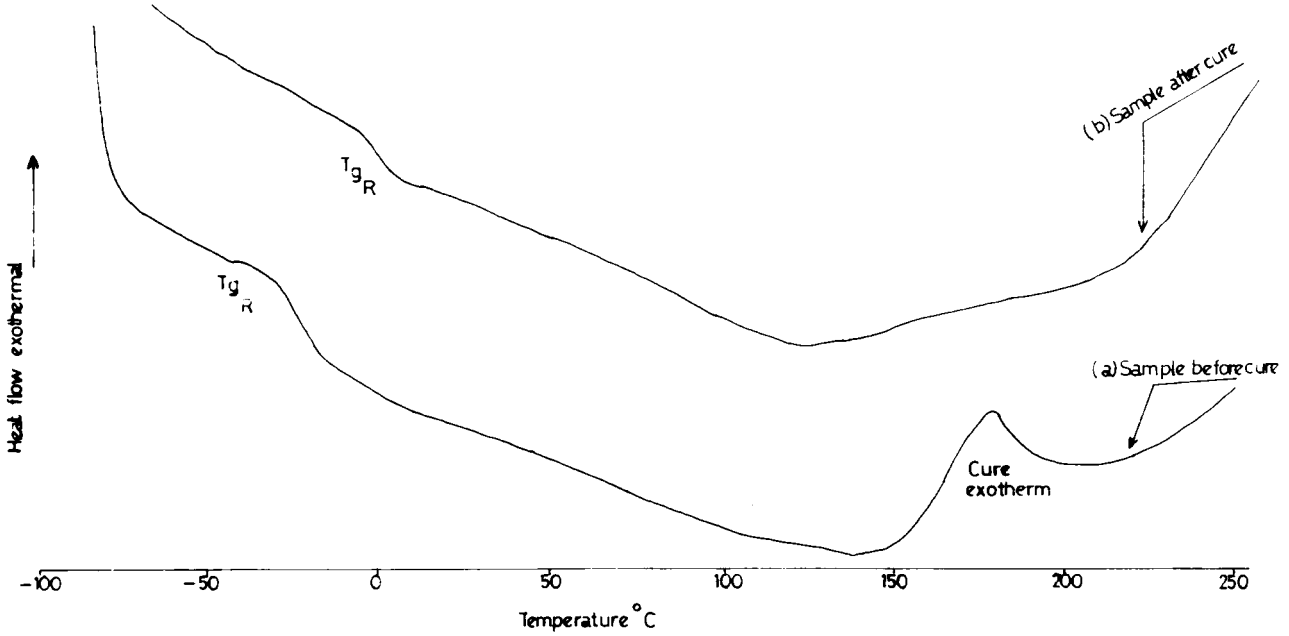

Figure 5 DSC trace of the nitrile–phenolic blend NBR/PCPF-b (50 : 50).

teristics, the observed mechanical behavior can be explained from this view point. PF and NBR, when mixed and heat cured, tend to separate into the component phases and form undesirably large domains.[13] It is likely that the interaction of PF resin with NBR is weak, and the low mechanical strength of the PF/NBR blend is presumably due to the inadequate adhesion between the phases. Strong adhesion between the phases can be achieved either by the addition of interfacial agents or by *in situ* reactive compatibilization.[28]

From the results reported in Table II, it can be realized that the relative crosslink density *Ve* of the rubber network in the blend increases as *p*-cresol content in the phenolic resin increases. It has been reported that nitrile rubbers can be vulcanized by *O*,*O'*dimethylol *p*-cresol through the reaction of quinone methide.[29,30] The chemical bonding across the rubber/phenolic resin interface improves the mechanical strength of the blend significantly by making the two phases to act as a unit rather than allowing them to respond separately to stress. The optimum value is the result of competition between the rubber–phenolic resin interface reaction, which tends to increase toughness and the increase in the number of crosslinks in the rubber, which presumably increases the solubility of rubber in the phenolic resin that eventually decrease the extensibility and the energy required for break.

Figure 8 shows the stress–strain properties of the PF/NBR and PCPF-c/NBR blends with 10, 20, 30, 40, and 50 wt % of added silica powder, which is used as filler for many applications of nitrile rubber and phenolic resin. Clearly, silica filler addition increases the modulus and decreases the ultimate strain (Fig. 8). In comparison to the PCPF-c/NBR blend, the elongation at break for the PF/NBR blend decreases dramatically as the silica filler content increases. The strength maximum for both the blends occurs at 30 wt % silica filler concentration.

The important parameters that control the mechanical behavior of polymer composites are the physicochemical properties of the constituents, polymer–filler interactions, the type of dispersion, the shape, size, and the content of filler.[31] Among these, the filler content is of cardinal importance and the optimum filler concentration is regarded as the limit of saturation of adsorption centers on the surface of the filler by the polymer molecules. For filler concentration greater than the optimum value, the filler particles are not perfectly wetted by the polymer molecules, which upset the continuity of the network structure and leads to strength deterioration. If the forces of attraction between the polymer molecule and filler are weaker than the intermolecular forces between the polymer molecules, the filler addition lowers the mechanical strength of the composite. So one must admit that there is strong interaction between the silica filler and the nitrile–phenolic

blend, and the interaction can occur in the rubbery phase as well as in the phenolic phase.

The SiO_2 surface is easily wetted with the nitrile–phenolic blend as the surface energy of silica is greater than that of the polymer. It can be realized that a considerable part of the chains of the special rubber network is adsorbed on the surface of the silica filler and the interaction leads to the increase in rubber crosslink density (Table II) and decrease in elongation of the composite (Fig. 3). Phenolic resin may chemisorb on the silica surface by the reaction of surface silanol (Si—OH) group with the methylol group of the phenolic resin. This leads us to believe that physically and chemically adsorbed layers of polymers around the silica filler surface create an interphase between the filler and the matrix phases. In composite systems, Hashin et al.[32] introduced the concept of a third phase (mesophase) that extend beyond a molecular layer interconnecting the two main phases (filler and matrix). This intermediate boundary layer also plays a role in the reinforcement of the composite and influence the mechanical strength. We believe that besides reinforcement the compatibilization of nitrile rubber, and phenolic resin is also achieved at the silica filler surface (discussed later).

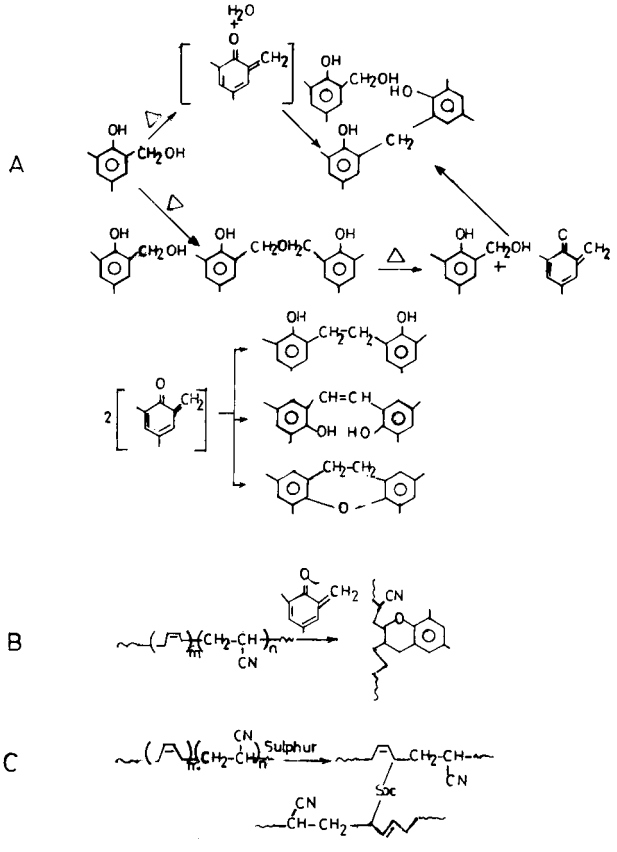

Figure 6 The chemical reactions that can occur during the cure of the nitrile–phenolic blend. (A) Self-hardening reaction of the phenolic resin. (B) Interlinking of the phenolic resin with NBR. (C) Vulcanization of NBR.

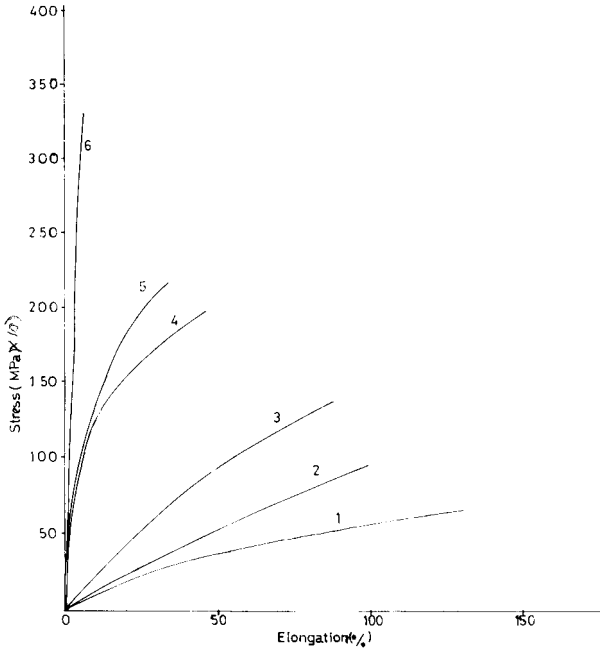

Figure 7 Stress–strain curves obtained with a 50 : 50 NBR/phenolic resin blend containing various *p*-cresol/phenol mol ratios in the phenolic resin: (1) NBR/PF; (2) NBR/PCPF-a; (3) NBR/PCPF-b; (4) NBR/PCPF-c; (5) NBR/PCPF-d; (6) NBR/PCF.

Adhesive Properties

Nitrile–phenolic blends form structural adhesives, which have a remarkable record of bond

Table II Energy Required for Break (E_b) (Area Under Stress–Strain Curve), Hardness and Relative Network Density (V_e) of Rubber in the Nitrile–Phenolic Blends

Sample Designation	E_b (J/mm^2)	Hardness (Shore D)	$V_e \times 10^5$ mol/mL
PF/NBR	0.202	27	75
	(0.253)	(52)	(83)
PCPF-a/NBR	0.251	32	78
PCPF-b/NBR	0.347	45	88
PCPF-c/NBR	0.360	49	126
	(0.463)	(69)	(196)
PCPF-d/NBR	0.282	59	216
PCF/NBR	0.140	62	236

The figures in the parenthesis are with 30 wt % silica filler.

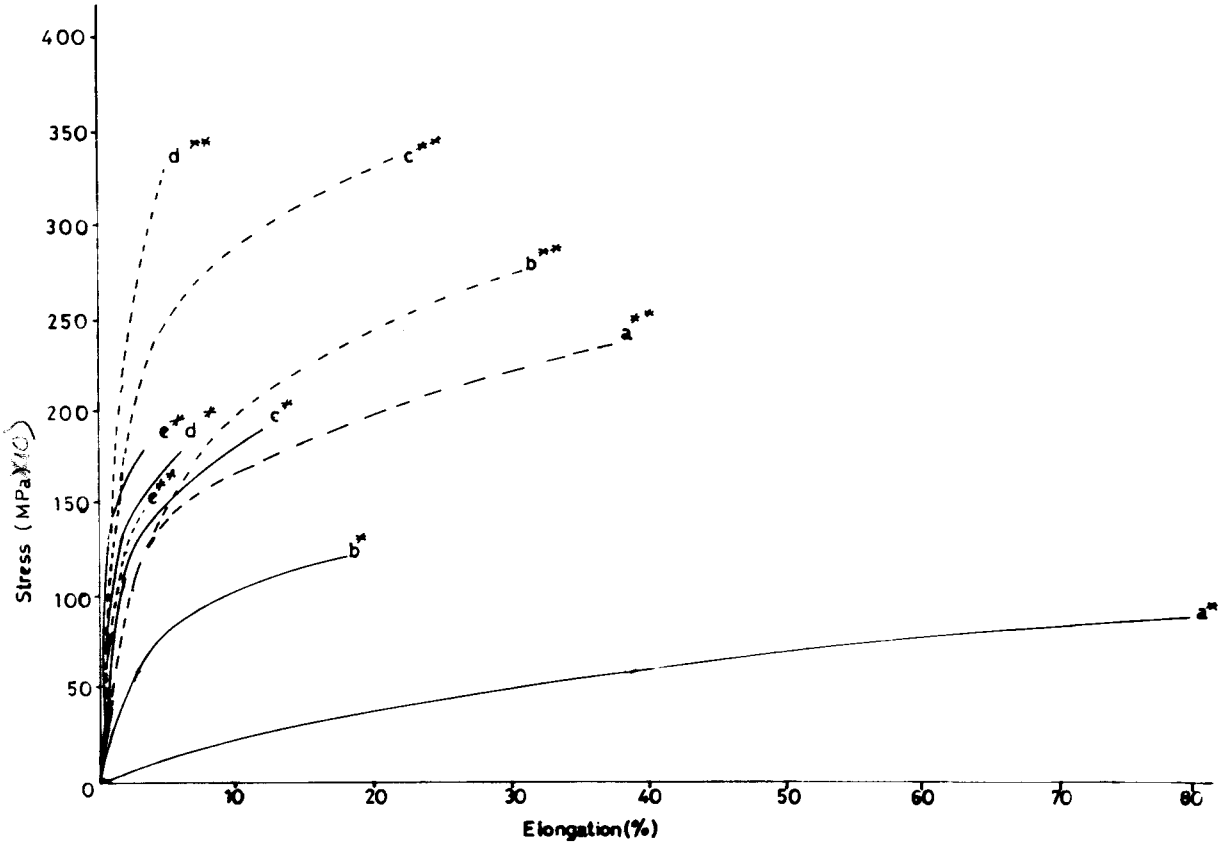

Figure 8 Dependence of stress–strain properties of nitrile–phenolic–silica composites on the silica content: (a, b, c, d, e) 10, 20, 30, 40, and 50 wt % silica, respectively; (*) NBR/PF; (**) NBR/PCPF-c.

durability to aluminium substrate.[3,4] The high adhesion of the nitrile–phenolic is believed to be due to the excellent wetting and chelate structure[10,33,34] formation of the phenolic component by the reaction of *O*-methyl hydroxyl phenol with aluminium oxide surface (Fig. 9). The joint strength of the nitrile–phenolic blend is also influenced with the rubber component that distributes the stress concentrations in the joint.

It is now agreed by most investigators that if satisfactory interfacial state of adhesion is achieved, the joint strength is closely related to the cohesive strength of the adhesive and the test parameters.[35–37] Table III gives the adhesive properties of nitrile–phenolic blends containing various PC/P mol ratios in the phenolic resin. It is evident from Table III that adhesive properties of the nitrile–phenolic blend increases (T-peel strength moderately decreases) with the increase of *p*-cresol (PC) concentration in the phenolic resin, and reaches a maximum at PC/P ratio 2 : 1 (PCPF-c). One may notice that adhesive strength of the blend is related to the stress–strain properties. Good lap shear strength seems to require an optimum combination of tensile strength, modulus, elongation, and high toughness (area under the stress–strain curve). For good T-peel strength, it would appear to require high toughness, low modulus, and high elongation. We believe that good adhesive properties of the NBR/PCPF-c blend is due to the higher toughness resulting from the increased interaction between the phenolic resin and the dispersed rubber

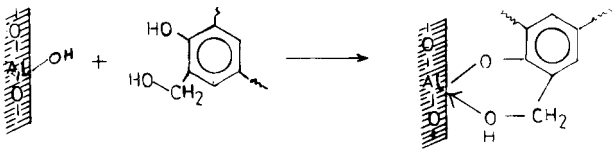

Figure 9 Possible reactions of phenolic resin with the aluminum oxide surface-forming chelate structure.

Table III Adhesive Properties of the Nitrile Rubber/Phenolic Resin (50 : 50) Blends

Sample Designation	Lap Shear Strength Al-to-Al (MPa)	T-Peel Strength Al-to-Al (kN/m)	180° Peel Strength Al-to-NBR (kN/m)
PF/NBR	6.8	2.0	2.2
	(9.0)	(1.3)	(2.5)
PCPF-a/NBR	11.8	1.8	4.5
PCPF-b/NBR	13.1	1.9	5.4
PCPF-c/NBR	16.4	1.7	7.6
	(17.2)	(0.9)	(7.1)
PCPF-d/NBR	15.3	1.1	5.5
PCF/NBR	4.9	0.8	0.6

The figures in parenthesis are with 30 wt % silica filler.

particles (mechanism previously explained). There is a decrease in the lap shear strength of the blend when the PC/P mol ratio in the phenolic resin is increased beyond 2 : 1, even though there is an increase in modulus and ultimate tensile strength. This is due to the higher stress at the edges of the lap joint and the inability of the adhesive to distribute stress evenly in the joint due to the brittleness. Some improvements in lap shear strength is observed by introducing silica filler into the nitrile–phenolic blends, and a plausible explanation is the decrease in internal stresses and increase in the cohesive strength.

It is evident from Table III that incorporation of *p*-cresol into the phenolic resin increases metal-to-rubber (NBR) peel strength, and the most improvement is observed for the NBR/PCPF-c blend. The superior metal-to-NBR peel strength exhibited by NBR/PCPF-c can be explained by the formation of a crossbridge between the elastomer and the adhesive due to the diffusion and interfacial reactivity. The mechanism of adhesive bonding of rubber-to-metal by nitrile–phenolics will be described in a subsequent article.[38] Poor peel strength exhibited by the PCF/NBR blend with metal/adhesive interface failure can be attributed to the over penetration of the adhesive into the elastomer, leading to a starved glue line.

Thermal Behavior

Thermal behavior of the nitrile–phenolic blends were studied by DSC and TGA from the view point of glass transition temperature (T_g) and thermal decomposition characteristics, and the results are listed in Table IV. The DSC thermogram of the blends indicates an endothermic shift in the baseline corresponding to the glass transition temperature of the nitrile rubber (typical DSC thermogram is shown in Fig. 5). No sign of glass transition corresponding to the phenolic part is obtained in the DSC thermogram, and this might be due to its highly crosslinked rigid structure. The pure NBR exhibits a T_g at −21°C, and in the PF/NBR blend no shift is observed for the T_g of the NBR component, indicating phase separation and incompatibility between the components. As phenol is replaced by *p*-cresol in the phenolic resin, the T_g of the NBR component in the blend shows a shift towards a higher temperature (Table IV). This effect is thought to be due to the greater phase mixing and chemical crosslinking between the NBR and phenolic resin. It is believed that phenolic resin with a high *p*-cresol content reacts

Table IV Rubber Glass Transition (T_{g_R}) and Thermal Decomposition Characteristics of Nitrile Rubber/Phenolic Resin (50 : 50) Blends

Sample Designation	T_{g_R} °(C)	T_i °(C)	T_{max} °(C)	T_f °(c)	Residue at 900°(C) (%)
PF/NBR	−21.5	420	480	520	22
	(−15.8)	(440)	(505)	(520)	(23)[a]
PCPF-a/NBR	−16.0	435	490	513	23
PCPF-b/NBR	−3.2	420	495	530	18
PCPF-c/NBR	14.8	430	470	510	19
	(38)	(435)	(469)	(520)	(21)[a]
PCPF-d/NBR	42.0	430	472	520	18
PCF/NBR	62.0	440	480	515	16

The figures in parenthesis are with 30 wt % silica filler.
[a] Residue calculated on a silica free basis.

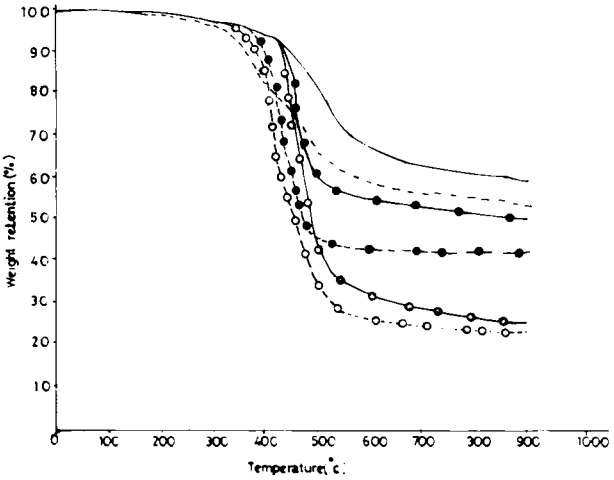

Figure 10 TG plots of cured samples. (——) PF resin, (----) PCPF-c resin; (— ○ —) NBR/PF (50 : 50), (--- ○ ---)NBR/PCPF-c (50 : 50); (— ● —) NBR/PF/ silica composite (30 wt % silica); (--- ● ---) NBR/ PCPF-c silica composite (30 wt % silica).

faster with NBR and act as a compatibilizing agent, anchoring the interface between the rubber particles and the phenolic matrix. This effect can lead to more homogenization and better adhesion between the two phases, resulting in improved mechanical properties.[39]

DSC results indicate that the presence of silica filler shifts the T_g of the NBR component in the blend to a higher temperature. The T_g of NBR component in the PF/NBR blend and the PCPF-c/NBR blend without and with silica filler (30 wt %) is shown in Table IV. The effect that shifts

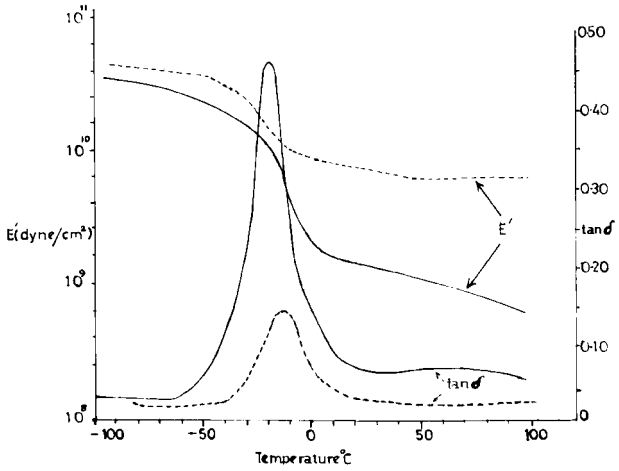

Figure 11 Dynamic mechanical spectra of the NBR/ PF blend: (——) without silica filler; (-----) with 30 wt % silica filler.

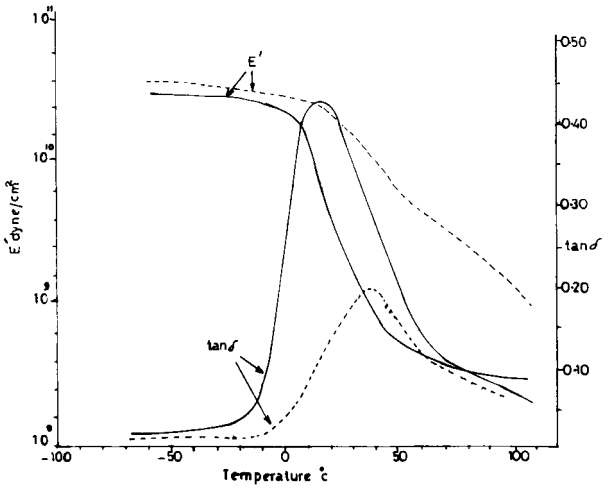

Figure 12 Dynamic mechnical spectra of the NBR/ PCPF-c blend: (——) without silica filler; (----) with 30 wt % silica filler.

the T_g of NBR component in the blend with the addition of silica filler can be surface compatibilization through the interaction of both the blend components with the filler surface.[40,41] With the assumption that both phenolic resin and nitrile rubber interact with the silica surface independently, the interphase compatibilization is achieved near the filler surface.

The thermal stability of the cured nitrile–phenolic blend was studied by thermogravimetry in N_2 and the onset or initial decomposition temperature (T_i), the maximum decomposition temperature (T_{max}), and the residue at 900°C are presented in Table IV. Figure 10 shows the comparative TG plots of cured samples of PF/NBR and PCPF–c/NBR blends without and with silica filler (30 wt %) and for the respective phenolic resins. The results in Table IV and Figure 10 indicate that the incorporation of *p*-cresol into the phenolics increases the thermal stability of the blend compared with the respective pure phenolics (Table I). This increase in the thermal stability of the blends may be due to the increase in crosslink density of the rubber, which is due to the increase in compatibility and bonding between the phenolic resin and NBR. It can be observed that the silica-filled nitrile–phenolic blend composite showed marginally higher thermal stability than the unfilled blend.

Figures 11 and 12 show the temperature dependence of storage modulus E' and damping tan δ over the temperature range −100 to +100°C for NBR/PF and NBR/PCPF-c blends without and with silica filler. Dynamic mechanical spectra of

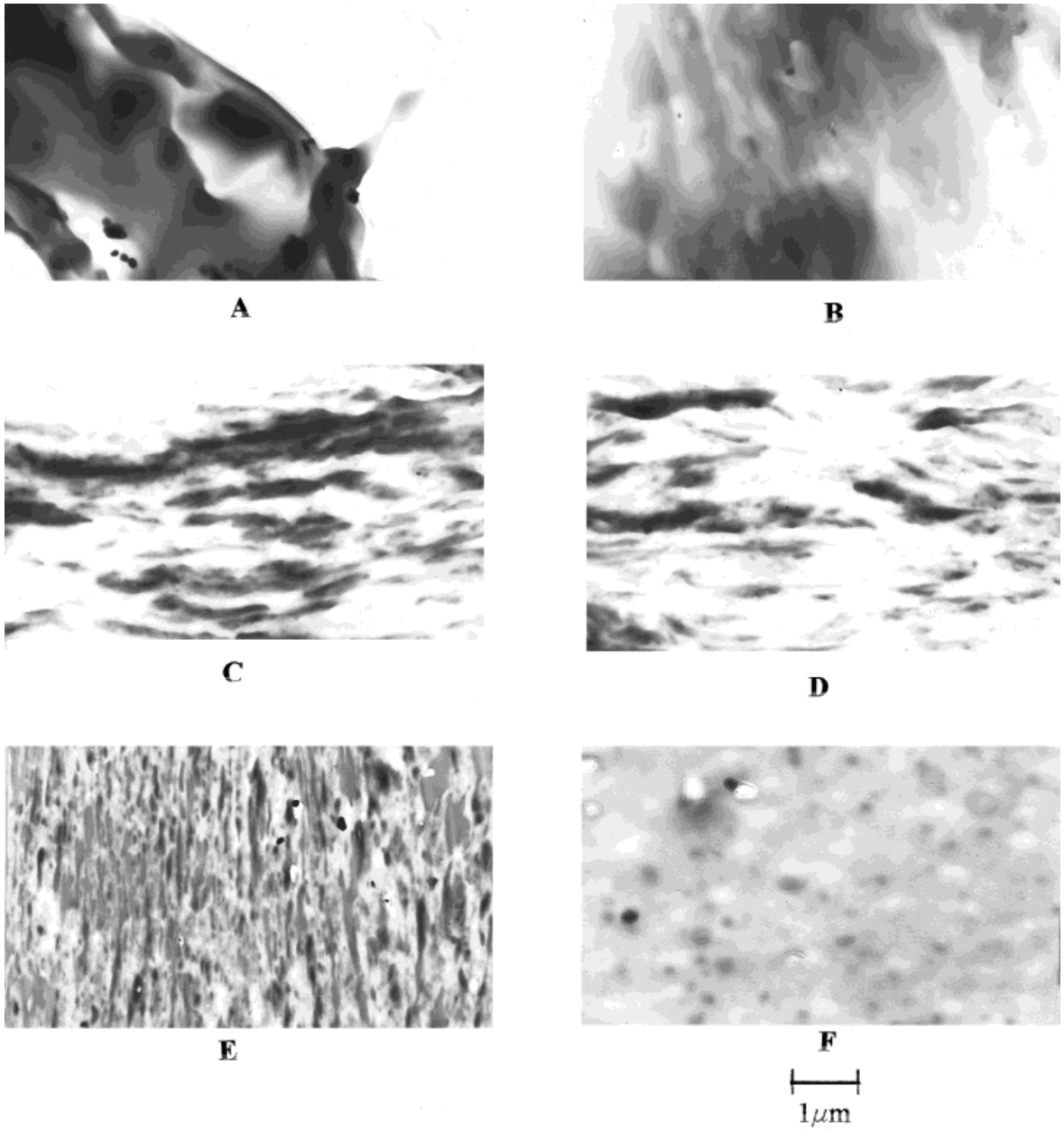

Figure 13 TEM micrographs of microtomed section of OsO_4-stained blends (NBR/phenolic resin 50 : 50). (A) NBR/PF, (B) NBR/PCPF-a, (C) NBR/PCPF-b, (D) NBR/PCPF-c, (E) NBR/PCPF-d, and (F) NBR/PCF.

the blends exhibit a drop in storage modulus E' and a maximum in tan δ corresponding to the glass transition temperature of the rubber network (T_{gR}). The E' of the rubbery region in the NBR/PCPF-c blend is higher than the NBR/PF blend. The tan δ peak of the rubbery region in the NBR/PCPF-c blend is shifted to a higher temperature and is broader than that in the NBR/PF blend. This indicates that the degree of compatibility and crosslinking of the rubber network is greater[42] in the NBR/PCPF-c blend compared with the NBR/PF blend. This agrees with the argument that PF resin has lower affinity for NBR, and *p*-cresol phenol formaldehyde establishes a strong interfacial adhesion with NBR through chemical reactions. Dynamic mechanical spectra of unfilled and SiO_2-filled nitrile–phenolic blends show that, with the SiO_2 filler the storage modu-

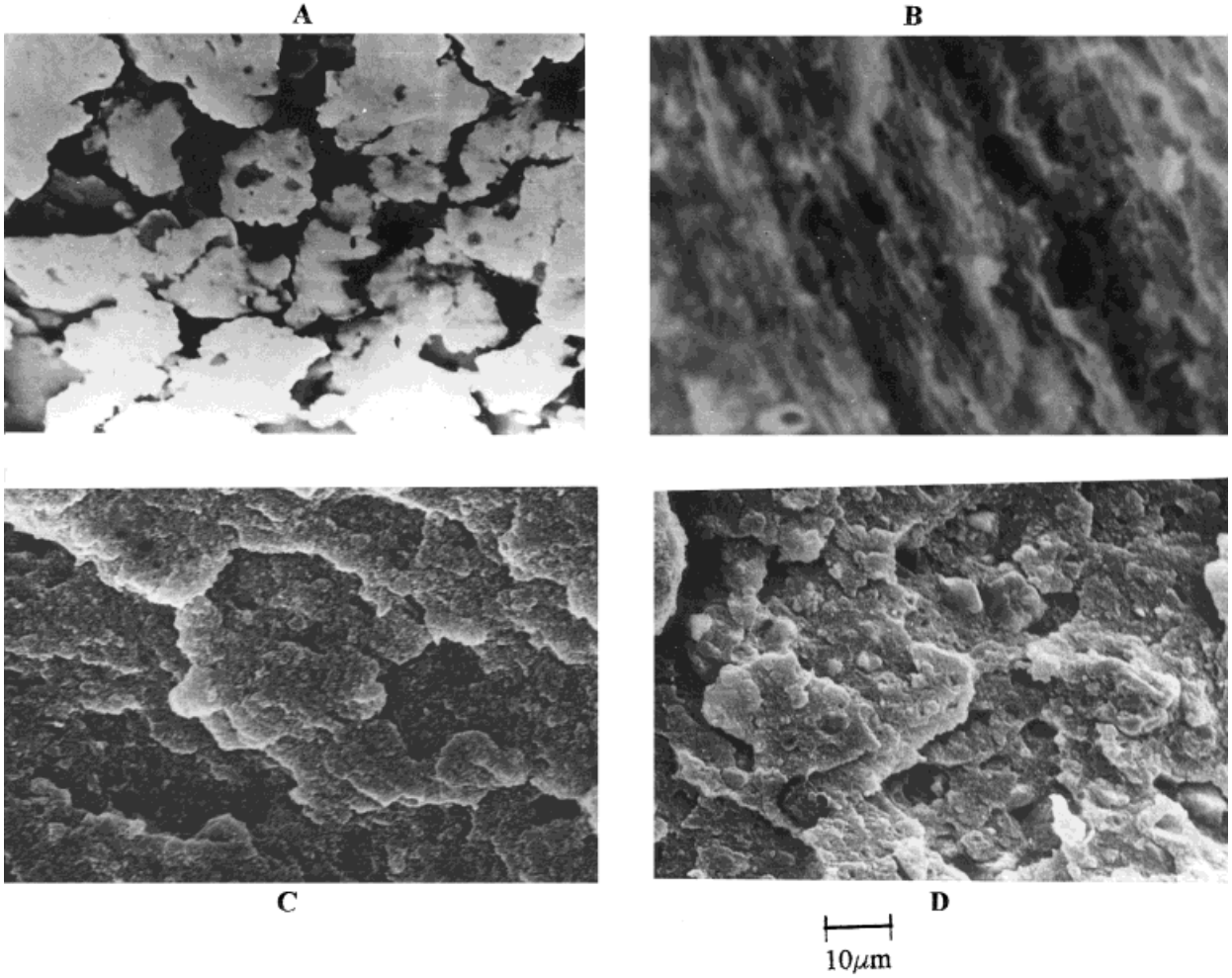

Figure 14 SEM micrographs of tensile-fractured surfaces of nitrile–phenolic blends. (A) NBR/PF, (B) NBR/PCPF-c, (C) NBR/PF with 30 wt % silica, and (D) NBR/PCPF-c with 30 wt % silica filler.

lus E' raises and tan δ height decreases, broadens, and shifts to a higher temperature. This behavior suggests that reinforcement and surface compatibilization occur because of the interaction of the blend component with the silica filler surface.

Morphology as Observed by TEM and SEM

The morphology of the blends was characterized by TEM and SEM studies (Figs. 13 and 14), which show phase separation. The dark regions in the TEM micrographs correspond to the rubber zone stained with OsO_4. Rubber particles are observed to contain spots, and may be due to the zinc oxide that plays the role of activator in the vulcanization of rubber. Larger size and irregularities in the shape of the rubber particles with clear phase boundaries reveal that PF/NBR is an incompatible blend [Figs. 13(A) and 14(A)]. *p*-Cresol modification remarkably improves compatibility between the NBR and phenolic resin, resulting in the formation of a smaller and more homogeneously distributed rubber domains having no clear phase boundaries. In the TEM photographs, finer dispersions of dark rubber domains appear within the lighter phenolic resin in the *p*-cresol–modified blends. This provides evidence for a greater level of miscibility and phase continuity, which can be ascribed to the increased interfacial interactions due to rubber/phenolic chemical reactions during cure. The extent of reaction between rubber and phenolic resin is expected to increase with increasing *p*-cresol content in the phenolic resin. TEM photos of the blends shown as a function of *p*-cresol content

in the phenolic resin (Fig. 13) reveal that at the highest *p*-cresol content instead of having a distinct separate phase, a continuous microphase results.

The rubber–phenolic resin reaction establishes crosslinking in the rubber, and the high strength of the *p*-cresol modified blends in comparison to the PF/NBR blend may be attributed to the interlocking of phases into three-dimensional networks. Comparison of Figure 14(A) and (B) leads to the conclusion that comparatively less interlocking of rubber particles is observed in the PF/NBR blend. Figure 14 shows the scanning electron micrographs of the fractured surface of unfilled and 30 wt % silica filled PF/NBR and PCPF-c/NBR blends. As seen in Figure 14, the rubber and phenolic resin are well bonded to the silica surface and a surface-induced compatibilization of the PF/NBR blend is evidenced in the SEM photo.

CONCLUSIONS

Phenolic resins of various *p*-cresol/phenol mol ratios were prepared, and the stress–strain, adhesive, thermal, and morphological properties of the cured phenolic resin/nitrile rubber (50 : 50) blends were studied with and without silica filler. Based on the results the following conclusions are drawn.

1. Incorporation of *p*-cresol into the phenolic resin improves the adhesive and mechanical properties of the phenolic resin/nitrile rubber blend, and the properties can be tailored easily to suit a particular application.
2. Replacing of phenol with *p*-cresol in phenolic resin enhances the interfacial adhesion of the NBR/phenolic resin phase and results in finer and diffused phase morphology. Reactive compatibilization seems to be the mechanism for the enhanced miscibility and strong interfacial adhesion of the phases.
3. *p*-Cresol modification of the phenolic resin introduces a certain amount of thermal stability to its blend with nitrile rubber. The glass transition temperature (T_{g_R}) of the NBR component in the blend is shifted towards a higher temperature. The insertion of crosslinking at the NBR/phenolic resin interphase is the main factor influencing the properties.
4. The addition of silica filler improves the modulus, ultimate tensile strength, and thermal performance of the nitrile–phenolic blend. Silica filler behaves both as a reinforcement and as a surface compatibilizer due to its interactions with the blend components at the surface.

The authors gratefully thank Dr. K. N. Ninan, Group Director, PSCG and Dr. V. N. Krishnamurthy, Deputy Director, PCM for the encouragement given during this work, and the Director, VSSC for the permission to publish this article. The authors are also thankful to their colleagues of ASD and PED for recording the thermograms and for carrying out the tests in Instron.

REFERENCES

1. D. R. Paul and J. W. Barlow, in *Multiphase Polymers,* S. L. Cooper and G. M. Estes, Eds., Advances in Chemistry Series 176, American Chemical Society, Washington, DC, 1979, p. 315.
2. H. C. Engel, WARD Tech. Report, 1952, p. 52.
3. N. J. DeLollis, *Adhesives, Adherend, Adhesion,* Kienger Publishing Company Inc., New York, 1980, p. 105.
4. J. D. Minford, *Handbook of Aluminium Bonding Technology Data,* Marcel Dekker, Inc., New York, 1993, p. 130.
5. J. Borowitz and R. Kosfeld, *Angew. Macromol. Chem.,* **100,** 23 (1981).
6. P. Sasidharan Achary and R. Ramaswamy, in *Proceedings of International Conference on Rubber and Rubber-Like Materials,* Rubber Technology Centre, Indian Institute of Technology, Kharagpur, India, 1986, p. 182.
7. P. Sasidharan Achary and R. Ramaswamy, in *Proceedings of Seminar on Science and Technology of Composites, Adhesives, Sealants,* Hindustan Aeronautics Ltd, Bangalor, India, 1989, p. 229.
8. P. Sasidharan Achary and R. Ramaswamy, *Chemical Weekly* (supplement on speciality chemicals) 78 (1991).
9. A. W. Birley, R. J. Heath, and M. J. Scott, *Plastic Materials Properties and Applications,* 2nd ed., Champan and Hall, New York, 1988, p. 149.
10. R. Ramaswamy and P. Sasidharan Achary, in *Adhesive Joints, Formation, Characteristics and Testing,* K. L. Mittal, Ed., Plenum Press, New York, 1984, p. 31.
11. H. Kollek, *Int. J. Adhesion Adhesives,* **5,** 75 (1985).
12. S. Wu, in *Polymer Blends,* vol. I, D. R. Paul and S. Newman, Eds., Academic Press, New York, 1978, p. 243.
13. P. Sasidharan Achary, G. Chockalingam, and R. Ramaswamy, *J. Adhesion Sci. Technol.,* **6,** 415 (1988).

14. P. Sasidharan Achary and R. Ramaswamy, *J. Adhesion Sci. Technol.,* **3,** 587 (1989).
15. D. R. Paul and S. Newman, *Polymer Blends,* vol. II, Academic Press, New York, 1978, p. 9.
16. J. T. Martin, in *Adhesion and Adhesives,* R. Houwink and G. Salomon, Eds., Elsevier Publishers, Amsterdam, 1065, p. 89.
17. G. M. Bristow and W. F. Waston, *Trans. Faraday Soc.,* **54,** 1731 (1958).
18. L. R. G. Treloar, *The Physics of Rubber Elasticity,* Clarendon Press, Oxford, 1975, p. 142.
19. B. Ellis and G. N. Welding, *Technique of Polymer Science,* Society of Chemical Industry, London, 1975, p. 46.
20. M. F. G. Loustalot et al., *Polymer,* **35,** 3048 (1994).
21. R. W. Lenz, *Organic Chemistry of Synthetic High Polymers,* Interscience, New York 1968, p. 133.
22. A. Zinke, *J. Appl. Chem.,* **1,** 257 (1951).
23. H. Tencher, D. Dobrev, and A Badev, *Angew. Macromol. Chem.,* **108,** 61 (1982).
24. A. Greeth, *Kuntstoffee,* **31,** 345 (1941).
25. K. Huttzsch, *J. Prakt. Chem.,* **158,** 275 (1941).
26. S. Van der Meer, *Rubber Chem. Technol.,* **18,** 853 (1945).
27. R. P. Lattimer, *Rubber Chem. Technol.,* **62,** 107 (1989).
28. M. Saleem and W. E. Baker, *J. Appl. Polym. Sci.,* **39,** 655 (1990).
29. W. J. S. Nauton, *The Applied Science of Rubber,* Edward Arnold Ltd., London, 1961, p. 137.
30. S. Van deer Meer. *Rev. Gen Coutch,* **20,** 230 (1943).
31. A. Voet, *J. Polym. Sci., Macromol. Rev.,* **15,** 327 (1980).
32. Z. Hashin and B. W. Rosen, *J. Appl. Mech.,* **31,** 223 (1964).
33. W. Brockmann, *Adhesive Age,* **20,** 30 (1977).
34. R. J. Turner, N. M. D. Brown, and D. G. Walmslen, *Vacuum,* **31,** 603 (1981).
35. K. L. Mittal, *Adhesion Measurement of Thin Films, Thick Films and Bulk Coatings,* ASTM STP 640, Philadelphia, 1978, p. 5.
36. A. F. Lewis and R. Saxon, in *Epoxy Resins, Chemistry and Technology,* C. A. May and Y. Tanaka, Eds., Marcel Dekker, New York, 1973, p. 373.
37. R. Ramaswamy and P. Sasidharan Achary, *J. Adhesion,* **11,** 305 (1981).
38. P. Sasidharan Achary, C. Gouri, and R. Ramaswamy, in preparation.
39. R. E. Cohen and A. R. Ramos, *Macromolecules,* **12,** 131 (1979).
40. Y. S. Liptov, in *Controlled Interphase in Composite Materials,* H. Ishida, Ed., Elsevier, New York, 1990, p. 599.
41. E. Morales, C. R. Herreoro, and J. L. Acosta, *Polym. Bull.,* **25,** 391 (1991).
42. C. B. Bucknall, *Toughened Plastics, Materials Science Series,* L. Holiday and A. Kelley, Eds., Applied Science Publishers, London, 1977, p. 1.